

# Neuropathological correlates of dopaminergic imaging in Alzheimer's disease and Lewy body dementias

Sean J. Colloby, Shane McParland, John T. O'Brien and Johannes Attems

Institute for Ageing and Health, Newcastle University, Campus for Ageing and Vitality, Newcastle upon Tyne, NE4 5PL UK

Correspondence to: Sean J. Colloby, PhD,  
Institute for Ageing and Health,  
Campus for Ageing and Vitality,  
Newcastle University,  
Newcastle upon Tyne,  
NE4 5PL, UK  
E-mail: s.j.colloby@ncl.ac.uk

Investigation of dopaminergic transporter loss *in vivo* using  $^{123}\text{I}$ -N-fluoropropyl-2 $\beta$ -carbomethoxy-3 $\beta$ -(4-iodophenyl) nortropane single photon emission computed tomography has been widely used as a diagnostic aid in Lewy body disease. However, it is not clear whether the pathological basis for the imaging changes observed reflects loss of dopaminergic transporter expressing neurons because of cell death or dysfunctional neurons due to possible nigral and/or striatal neurodegenerative pathology. We aimed to investigate the influence of nigral neuronal loss as well as nigral ( $\alpha$ -synuclein, tau) and striatal ( $\alpha$ -synuclein, tau, amyloid  $\beta$ ) pathology on striatal uptake in a cohort of autopsy-confirmed Alzheimer's disease ( $n = 4$ ), dementia with Lewy bodies ( $n = 7$ ) and Parkinson's disease dementia ( $n = 12$ ) cases. Subjects underwent ante-mortem dopaminergic scanning and post-mortem assessments (mean interval 3.7 years). Striatal binding (caudate, anterior and posterior putamen) was estimated using region of interest procedures while quantitative neuropathological measurements of  $\alpha$ -synuclein, tau and amyloid  $\beta$  were carried out. Similarly, nigral neuronal density was assessed quantitatively. Stepwise linear regression was performed to identify significant pathological predictors of striatal binding. In all striatal regions, image uptake was associated with nigral dopaminergic neuronal density ( $P \leq 0.04$ ) but not  $\alpha$ -synuclein ( $P \geq 0.46$ ), tau ( $P \geq 0.18$ ) or amyloid  $\beta$  ( $P \geq 0.22$ ) burden. The results suggest that reduced uptake *in vivo* may be influenced considerably by neuronal loss rather than the presence of pathological lesions, in particular those related to Alzheimer's disease and Lewy body dementias. However, dysfunctional nigral neurons may have an additional effect on striatal uptake *in vivo* but their respective role remains to be elucidated.

**Keywords:** Alzheimer's disease; dementia with Lewy bodies; Parkinson's disease dementia; striatum;  $^{123}\text{I}$ -FP-CIT; SPECT; neuropathology

**Abbreviations:** EDTA = Ethylenediaminetetraacetic acid; FP-CIT =  $^{123}\text{I}$ -N-fluoropropyl-2 $\beta$ -carbomethoxy-3 $\beta$ -(4-iodophenyl) nortropane; SPECT = single photon emission computed tomography; UPDRS = Unified Parkinson's Disease Rating Scale

## Introduction

Dementia with Lewy bodies is the second most common cause of neurodegenerative dementia following Alzheimer's disease

(Rahkonen *et al.*, 2003). It is characterized clinically by recurrent visual hallucinations, cognitive fluctuations and spontaneous motor parkinsonism (McKeith *et al.*, 2005). The development of dementia is a frequent complication of Parkinson's disease, occurring in

up to 6 times the rate of similarly aged healthy individuals (Emre *et al.*, 2007). Dementia with Lewy bodies and Parkinson's disease dementia have a similar clinical phenotype, the distinction of which is based on the timing of the onset of cognitive symptoms relative to motor symptoms ( $\leq 1$  year = dementia with Lewy bodies,  $> 1$  year = Parkinson's disease dementia; McKeith *et al.*, 2005).

Neuropathologically, Alzheimer's disease is characterized by the presence of extracellular amyloid-amyloid  $\beta$  aggregates as plaques, hyperphosphorylated microtubule associated protein tau (neurofibrillary tangles and neuropil threads) and neuritic plaques that are composed of both amyloid  $\beta$  and tau. Whilst in Alzheimer's disease these lesions occur primarily in limbic and neocortical regions, subcortical nuclei such as the substantia nigra become severely involved in later stages of the disease (Attems *et al.*, 2011). The extent and distribution of neurofibrillary tangles and neuropil threads in Alzheimer's disease have also been shown to correlate with dementia severity and duration of illness (Duyckaerts *et al.*, 2009; Perl, 2010). In dementia with Lewy bodies,  $\alpha$ -synuclein containing Lewy bodies and Lewy neurites are found in the brainstem (e.g. dorsal motor nucleus of vagal nerve, locus coeruleus and substantia nigra), the basal forebrain/limbic regions (e.g. nucleus basalis of Meynert, amygdala, transentorhinal cortex and cingulate cortex) and the neocortex (Braak *et al.*, 2003; McKeith *et al.*, 2005; Ferman and Boeve, 2007). Additional Alzheimer's disease pathology (i.e. amyloid  $\beta$  and tau) is frequently present in dementia with Lewy bodies to varying extent. Dementia severity in dementia with Lewy bodies has been shown to be associated with the severity of  $\alpha$ -synuclein but not of amyloid  $\beta$  or tau pathology, respectively (Samuel *et al.*, 1996; Hurtig *et al.*, 2000). In Parkinson's disease dementia, however, pathological findings are variable, with some reporting additional Alzheimer's disease as the cause for dementia (Libow *et al.*, 2009), while others have indicated limbic and cortical  $\alpha$ -synuclein pathology as the main substrate for dementia (Hurtig *et al.*, 2000; Aarsland *et al.*, 2005), where cognitive decline was shown to relate to density of cortical Lewy bodies (Aarsland *et al.*, 2005). In addition, others have revealed similar cortical  $\alpha$ -synuclein pathology between dementia with Lewy bodies and Parkinson's disease dementia (Tsuboi *et al.*, 2007). Lewy bodies have also been described in Alzheimer's disease but unlike dementia with Lewy bodies appear to be frequently confined to the amygdala (Hamilton, 2000; Sahin *et al.*, 2006; Tsuboi *et al.*, 2007).

The loss of dopaminergic neurons in the substantia nigra pars compacta that project to the striatum (nigrostriatal pathway) with presence of Lewy bodies in some of the remaining neurons and abundant Lewy neurites in the neuropil are common neuropathological features of Lewy body diseases (Schulz-Schaeffer, 2010). A significant burden of striatal Lewy body pathology has been observed in Parkinson's disease and to a greater extent in dementia with Lewy bodies (Duda *et al.*, 2002; Tsuboi *et al.*, 2007). Nigrostriatal dopaminergic function has also been assessed in Alzheimer's disease, dementia with Lewy bodies and Parkinson's disease dementia *in vivo* with single photon emission computed tomography (SPECT) and PET imaging. Using SPECT tracers,  $^{123}\text{I}$ -2 $\beta$ -carbomethoxy-3 $\beta$ -(4-iodophenyl) tropane ( $\beta$ -CIT) and  $^{123}\text{I}$ -*N*-fluoropropyl-2 $\beta$ -carbomethoxy-3 $\beta$ -(4-iodophenyl) nortropane (FP-CIT), significantly

reduced striatal dopamine transporter binding in dementia with Lewy bodies compared with Alzheimer's disease (Donnemiller *et al.*, 1997), as well as in dementia with Lewy bodies and Parkinson's disease dementia relative to Alzheimer's disease and healthy controls, respectively (Walker *et al.*, 2002; O'Brien *et al.*, 2004). Using PET, striatal  $^{18}\text{F}$ -fluorodopa uptake was shown to be decreased in dementia with Lewy bodies compared with Alzheimer's disease (Hu *et al.*, 2000), and in Parkinson's disease dementia relative to controls (Ito *et al.*, 2002). In addition, reduced striatal vesicular transporters have been observed in dementia with Lewy bodies compared with Alzheimer's disease and healthy controls using  $^{11}\text{C}$ -dihydrotrabenazine (Koeppel *et al.*, 2008). However, no previous validation of *in vivo* imaging as a marker for dopaminergic cell loss at autopsy has been undertaken. Indeed, few studies have investigated the relationship between neuropathology and neuroimaging changes in Alzheimer's disease, dementia with Lewy bodies and Parkinson's disease dementia. Previously, correlations between hippocampal volume and neurofibrillary tangles pathology were described in Alzheimer's disease using post-mortem (Huesgen *et al.*, 1993; Gosche *et al.*, 2002) and ante-mortem MRI (Jack *et al.*, 2002; Csernansky *et al.*, 2004). More recently, the association between volumetric MRI measures (hippocampus, amygdala and entorhinal cortex) and burden of neuropathology (amyloid  $\beta$ , tau and  $\alpha$ -synuclein) in those regions were studied in patients with pathological diagnosis of Lewy body disease (ante-mortem diagnosis: 14 dementia with Lewy bodies and nine Parkinson's disease dementia) (Burton *et al.*, 2012). Although nigral dopaminergic input to the striatum via the nigrostriatal pathway is linked to striatal function (Nicola *et al.*, 2000), it is unclear whether deficits in striatal binding observed on  $^{123}\text{I}$ -FP-CIT SPECT are associated with a loss of dopaminergic neurons and/or dysfunctional neurons (characterized by reduced amounts of the dopamine transporter rather than neuronal loss), which may be associated with  $\alpha$ -synuclein, tau and amyloid  $\beta$  pathology in selected brain regions. The aim of this study was to investigate the influence of nigral neuronal loss as well as nigral ( $\alpha$ -synuclein, tau) and striatal ( $\alpha$ -synuclein, tau and amyloid  $\beta$ ) pathology on striatal  $^{123}\text{I}$ -FP-CIT SPECT uptake in a cohort of autopsy-confirmed cases with Alzheimer's disease, dementia with Lewy bodies and Parkinson's disease dementia.

## Materials and methods

### Subjects

Subjects were selected from neuropathologically assessed cases in the Newcastle Brain Tissue Resource. The study was approved by the local ethics committee and UK Department of Health Administration of Radioactive Substances Advisory Committee. All participants gave informed written consent, and at death, their nearest relative gave permission for post-mortem examination and use of autopsy material and previous clinical data for research. All individuals during life had originally participated in a prospective longitudinal study of dementia and underwent clinical and cognitive testing including the Mini-Mental State Examination (Folstein *et al.*, 1975) and Cambridge Cognitive Examination (Roth *et al.*, 1986). Parkinsonism was assessed using the motor subsection of the Unified Parkinson's Disease Rating Scale

(UPDRS III; Fahn *et al.*, 1987). All subjects had at least one  $^{123}\text{I}$ -FP-CIT SPECT prior to death (mean interval = 3.8 years, range: 1.5–6.8 years) and were recruited from a community-dwelling population who had been referred to local old age psychiatry services. Ante-mortem diagnosis was made using the consensus criteria for Alzheimer's disease (McKhann *et al.*, 1984), dementia with Lewy bodies and Parkinson's disease dementia (McKeith *et al.*, 1996). Neuropathological assessment followed standardized criteria for the diagnosis of Alzheimer's disease (Mirra *et al.*, 1993; Hyman, 1998; Braak *et al.*, 2006) and for dementia with Lewy bodies/Parkinson's disease the staging/typing method suggested by Alafuzoff *et al.* (2009). Of note, cases with Parkinson's disease dementia that developed extrapyramidal symptoms for >1 year prior to the development of cognitive impairment fulfilled criteria for Parkinson's disease dementia. Clinically, there were three cases with Alzheimer's disease, eight with dementia with Lewy bodies and 12 cases with Parkinson's disease dementia, though final clinicopathological consensus diagnoses were four with Alzheimer's disease, seven dementia with Lewy bodies and 12 with Parkinson's disease dementia, the discrepancy due to the fact that one case with dementia with Lewy bodies ['possible' dementia with Lewy bodies diagnosis clinically, 'normal' (FP-CIT SPECT) uptake on visual rating] was neuropathologically diagnosed as Alzheimer's disease.

## $^{123}\text{I}$ -FP-CIT single photon emission computed tomography imaging

Subject scans were acquired on a triple-detector rotating gamma camera (Picker 3000XP) fitted with a low-energy high-resolution fan-beam collimator. Four hours after a bolus intravenous injection of 150 MBq (specific activity >100TBq/mmol) of  $^{123}\text{I}$ -FP-CIT (DaTSCAN, GE Healthcare), 120 15-s views over a 360° orbit were obtained from each detector on a 128 × 128 matrix with a pixel size and slice thickness of 3.5 mm. Imaging time was 30 min. Image reconstruction was performed using ramp-filtered back-projection with a Butterworth filter (order 13, cut-off 0.3 cycles/cm) to produce the transverse sections. The data were then resampled to generate 64 × 64 matrix images with 4.0 mm cubic voxels. Images were not corrected for gamma ray attenuation.

## $^{123}\text{I}$ -FP-CIT binding

A semi-automated region of interest analysis was performed on all  $^{123}\text{I}$ -FP-CIT SPECT imaging data in order to obtain right hemispheric estimates of specific to non-specific uptake ratios in caudate, anterior and posterior putamen for each subject. Total striatal activity ratios were also calculated in the right hemisphere from the average caudate, anterior and posterior putamen values. A more detailed description of the procedure has been previously reported (O'Brien *et al.*, 2004).

## Assessment of nigral and striatal pathology

### Histochemistry and immunohistochemistry

Following a standardized procedure for the sampling of the lower midbrain, tissue blocks containing the right substantia nigra were taken at the level of the third cranial nerve's exit in a horizontal plane. From the respective paraffin-embedded tissue blocks 6- $\mu\text{m}$  microtome sections were examined using Cresyl fast violet histochemistry for the visualization of cells and immunohistochemistry for the visualization of  $\alpha$ -synuclein (antibody  $\alpha$ -syn, Leica) and tau

(phosphorylated tau protein; antibody AT8, Autogenbioclear) pathology. Likewise 6- $\mu\text{m}$  microtome sections from paraffin-embedded tissue blocks that were taken in a frontal plane caudal/posterior to the optic chiasma containing caudate nucleus and putamen were incubated with both  $\alpha$ -syn and AT8 antibodies. In addition, for the visualization of amyloid  $\beta$  pathology (amyloid  $\beta$  plaques) those sections were incubated with an anti-amyloid  $\beta$  antibody raised against amyloid  $\beta_{17-24}$  (Clone 4G8, Signet Labs). For Cresyl fast violet staining, paraffin-embedded tissue was dewaxed, washed three times in distilled water, incubated in Cresyl fast violet, preheated to 60°C and removed from the incubator. Tissue was subsequently differentiated in 95% alcohol, dehydrated and mounted. Antigen unmasking for immunohistochemistry was performed by pressure cooking slides in 0.1 M ethylenediaminetetraacetic acid (EDTA) for 1 min 30 s ( $\alpha$ -syn) or microwaving in 0.01 M citrate buffer for 10 min (AT8), prior to incubation with the primary antibody. The immunoreactive product was then visualized by 3,3'-diaminobenzidine.

### Image analysis—quantification

Images from Cresyl fast violet,  $\alpha$ -syn and AT8 stained slides containing the substantia nigra were captured at ×100 magnification using a Nikon 90i microscope with DsFi1 camera coupled to a personal computer. For quantification of pigmented neurons,  $\alpha$ -syn and AT8 burden we used the NIS Elements image analysis system (Nikon). Figure 1 illustrates the assessment of number of pigmented neurons,  $\alpha$ -synuclein and tau pathology in the substantia nigra. To ensure that the entire substantia nigra present on the single section analysed could be assessed, nine adjacent images (rectangle of 3 × 3 images, large image acquisition) from each Cresyl fast violet,  $\alpha$ -syn and AT8 stained slides were taken at ×100 magnification and imported into the NIS Elements software, which added individual images into one single image representing an area of 1.62 × 2.12 mm<sup>2</sup> (Fig. 1B). The area of immunopositivity was measured in each of the three image acquisitions. Red–Green–Blue thresholds, which determine the pixels that are included in the binary layer used for measurement, were standardized separately for each neuronal stain (Cresyl fast violet), AT8 and  $\alpha$ -syn (Fig. 1C). In addition to Red–Green–Blue thresholds we set and standardized restriction thresholds that comprise a set of parameters to further define objects that are included in the final measurement (Fig. 1E, F and I). Restriction threshold applied for neurons (Cresyl fast violet stain) included the mean colour intensity typical for pigmented neurons and an object area of 40–700  $\mu\text{m}^2$ . The latter was necessary to ensure that small pigmented areas that might represent pigment incontinence were not counted as nigral neurons. A region of interest for measurement was manually drawn around the substantia nigra pars compacta, which was identified by the presence of pigmented neurons. Hence the regions of interest showed serrate or winding borders. Neuronal density in the substantia nigra was calculated by dividing neuronal numbers by region of interest area and stated as neurons per mm<sup>2</sup>. Separately for each  $\alpha$ -syn and AT8 restriction threshold included the mean colour intensity to define true immunopositive structures [ $<184$  SI units (max 255), Fig. 1G]. Regions of interest around the substantia nigra matched the ones determined for corresponding Cresyl fast violet slides and the area covered by AT8 and  $\alpha$ -syn immunohistochemical signals gave percentage of area covered by tau and  $\alpha$ -synuclein pathology, respectively.

For the assessment of  $\alpha$ -syn, AT8 and 4G8 immunopositivity in the caudate nucleus and putamen, three randomly allocated large image acquisitions from each caudate nucleus and putamen were captured (see Fig. 2 for description).

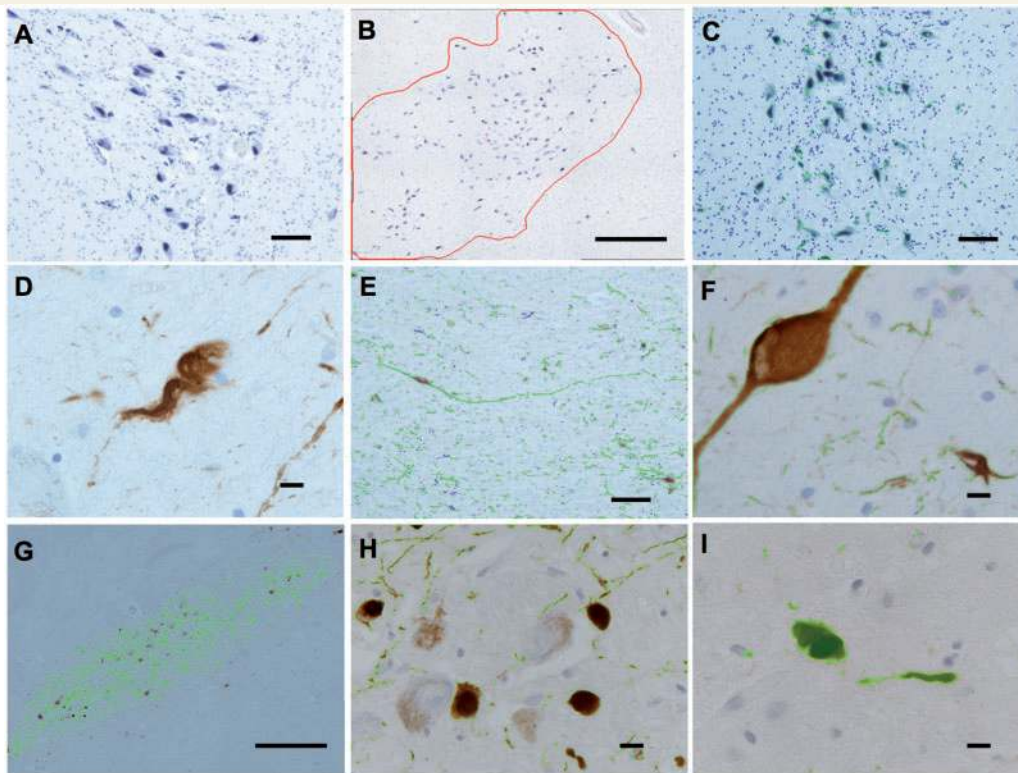


**Figure 1** Assessment of number of pigmented neurons,  $\alpha$ -synuclein and tau pathology in the substantia nigra. For each assessment nine individual images were taken at  $\times 100$  magnification (A, histochemistry for Cresyl fast violet) and added to one single image that included the entire substantia nigra pars compacta (B). Regions of interest were manually identified (red line in B). On histochemical (Cresyl fast violet, A) and immunohistochemical (AT8, D–F;  $\alpha$ -syn, G–I) images, standardized Red–Green–Blue thresholds were set to produce binary images (Cresyl fast violet, B and C; AT8, E and F;  $\alpha$ -syn, G–I) on which standardized restriction thresholds (for details see ‘Materials and methods’ section) determined the objects to be measured; green lines encircle nigral neurons in (C) and indicate the objects counted to quantify the number of nigral neurons. Neuropil threads or neurofibrillary tangles (tau pathology; E and F) and Lewy neurites or Lewy bodies ( $\alpha$ -synuclein pathology; G–H) are delineated by green lines, indicating the areas that were added for the calculation of the total area covered by AT8 and  $\alpha$ -syn immunopositivity, respectively. For clarification, these areas are shaded in green in (I). Staining: Cresyl fast violet (CFV), (A–C); AT8 (D–F);  $\alpha$ -syn (G–I). Scale bars = 0.1 mm (A, C, E, G and H), 0.5 mm (B) and 0.01 mm (D, F and I).

## Statistical analysis

The Statistical Package for Social Sciences software (SPSS ver. 19; <http://www-01.ibm.com/software/analytics/spss/>) was used for statistical evaluation. Continuous variables were tested for normality of distribution using the Shapiro–Wilk test and visual inspection of variable histograms. Group differences in subject characteristics, SPECT binding ratios and neuropathological measures were assessed using *F*-tests (ANOVA) while for categorical variables  $\chi^2$  tests were used. Stepwise linear regression analysis was performed to identify significant pathological predictors of striatal  $^{123}\text{I}$ -FP-CIT binding across the entire study sample (Alzheimer’s disease, dementia with Lewy bodies and Parkinson’s disease dementia combined). Partial correlation coefficients (*r*) were then used to examine the strength of association between the significant predictors and striatal binding variables controlling for interval between SPECT scan and death, and  $^{123}\text{I}$ -FP-CIT per cent annual rate of decline (results of which were obtained from a previous longitudinal FP-CIT study of dementia; Colloby *et al.*, 2005). Age, cognitive and clinical effects on FP-CIT imaging and pathological variables were examined by Pearson’s correlation coefficients (*r*). For correlation analyses, all reported *P*-values were corrected for family-wise error rates (Bonferroni). A *P*-value

$<0.05$  was considered significant. To investigate the reliability of all pathological measurements, the same examiner (S.M.) assessed seven randomly selected cases on three separate occasions (identical subjects), 1 day apart. To evaluate the extent to which measurements were consistent over time (test–retest reliability), intraclass correlation coefficients were calculated (two-way mixed effects model) with 95% confidence intervals (CIs).

## Results

### Subjects

Table 1 summarizes the group characteristics. Groups were comparable for gender, age at SPECT, interval between SPECT and death, disease duration at death as well as Mini-Mental State Examination and Cambridge Cognitive Examination both at SPECT and last assessment ( $P \geq 0.05$ ). Age at death was higher in Alzheimer’s disease than in Parkinson’s disease dementia ( $P = 0.02$ ), while Parkinson’s disease dementia also had longer disease duration at SPECT than dementia with Lewy bodies

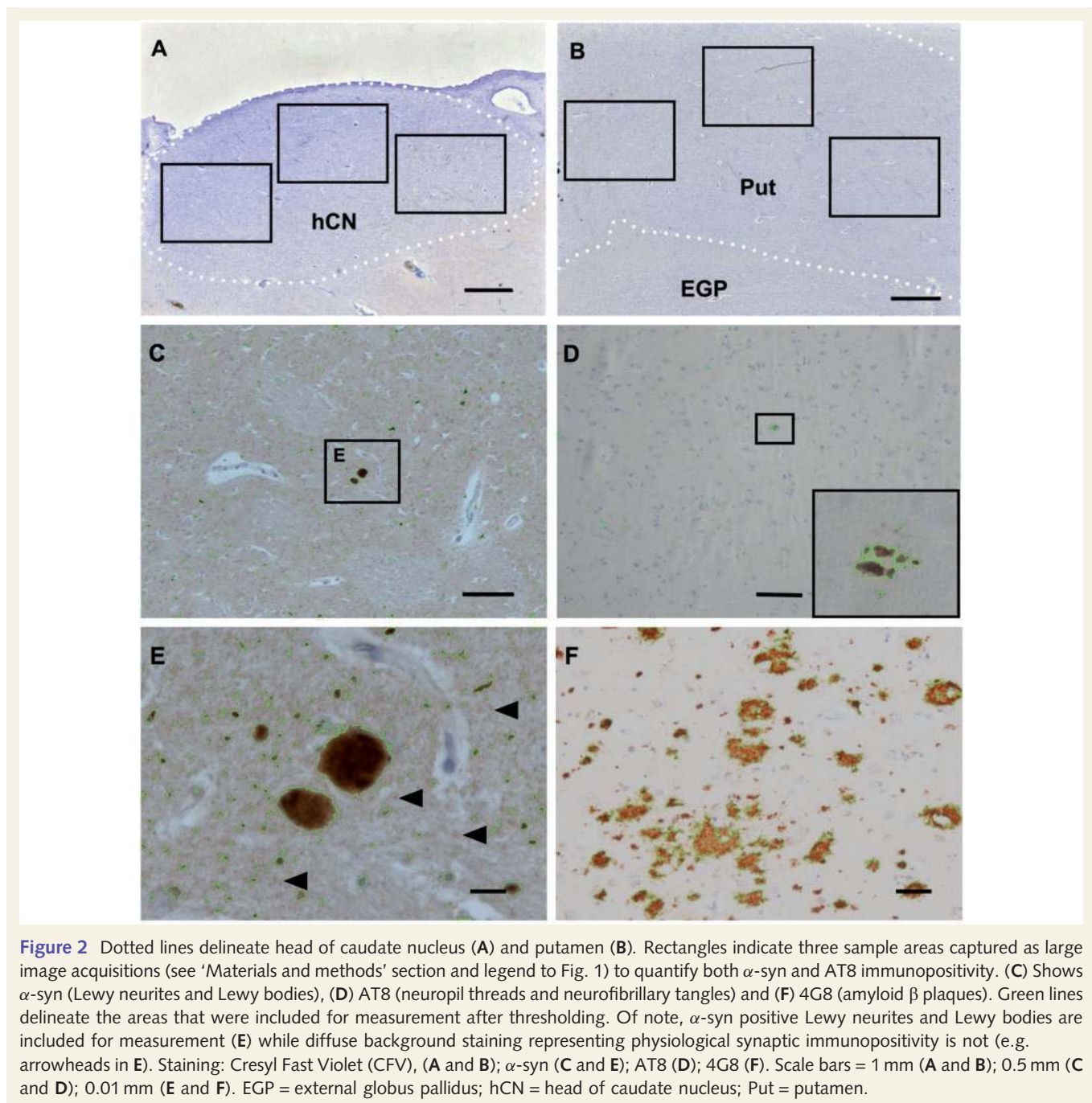


**Figure 2** Dotted lines delineate head of caudate nucleus (A) and putamen (B). Rectangles indicate three sample areas captured as large image acquisitions (see 'Materials and methods' section and legend to Fig. 1) to quantify both  $\alpha$ -syn and AT8 immunopositivity. (C) Shows  $\alpha$ -syn (Lewy neurites and Lewy bodies), (D) AT8 (neuropil threads and neurofibrillary tangles) and (F) 4G8 (amyloid  $\beta$  plaques). Green lines delineate the areas that were included for measurement after thresholding. Of note,  $\alpha$ -syn positive Lewy neurites and Lewy bodies are included for measurement (E) while diffuse background staining representing physiological synaptic immunopositivity is not (e.g. arrowheads in E). Staining: Cresyl Fast Violet (CFV), (A and B);  $\alpha$ -syn (C and E); AT8 (D); 4G8 (F). Scale bars = 1 mm (A and B); 0.5 mm (C and D); 0.01 mm (E and F). EGP = external globus pallidus; hCN = head of caudate nucleus; Put = putamen.

( $P = 0.04$ ). As expected, those with Parkinson's disease dementia had higher UPDRS III scores at SPECT and at last assessment than subjects with Alzheimer's disease, but no significant differences were observed between those with dementia with Lewy bodies and Parkinson's disease dementia ( $P \geq 0.06$ ).

### **$^{123}\text{I}$ -FP-CIT single photon emission computed tomography activity ratios—right hemisphere**

Table 2 depicts the mean  $^{123}\text{I}$ -FP-CIT SPECT binding ratios in Alzheimer's disease, dementia with Lewy bodies and Parkinson's

disease dementia. During life, significant differences in uptake were observed between groups in caudate, anterior putamen, posterior putamen and striatum ( $P < 0.003$ ). In all regions, significantly lower uptake was apparent in Parkinson's disease dementia compared with both Alzheimer's disease and dementia with Lewy bodies ( $P < 0.04$ ). FP-CIT annual rates of decline expressed as per cent of baseline value are also presented for each region of interest, data from Colloby *et al.* (2005) (Table 2). Rates did not significantly differ between groups in anterior and posterior putamen as well as whole striatum ( $P > 0.1$ ); however, in caudate, rates in Parkinson's disease dementia were greater than in Alzheimer's disease and dementia with Lewy

**Table 1 Subject characteristics**

Characteristic	Alzheimer's disease	Dementia with Lewy bodies	Parkinson's disease dementia	P-value
<i>n</i>	4	7	12	
Gender (male:female)	3:1	4:3	10:2	$\chi^2 = 1.6, P = 0.5$
Age at SPECT (years)	79.3 ± 6.3	76.4 ± 8.5	70.8 ± 4.3	$F(2,20) = 3.7, P = 0.05$
Age at death (years)	83.8 ± 6.0	79.9 ± 7.4	74.1 ± 4.2	$F(2,20) = 5.3, P = 0.01^a$
Interval between SPECT and death (years)	4.6 ± 0.5	3.5 ± 1.7	3.3 ± 1.7	$F(2,20) = 0.9, P = 0.4$
Disease duration at SPECT (years)	2.5 ± 2.0	1.9 ± 1.2	7.9 ± 6.3	$F(2,20) = 4.2, P = 0.03^b$
Disease duration at death (years)	7.2 ± 2.1	5.5 ± 2.5	11.5 ± 6.1	$F(2,20) = 3.6, P = 0.05$
UPDRS III at SPECT	8.5 ± 4.0	21.4 ± 15.3	35.8 ± 11.9	$F(2,20) = 8.3, P = 0.002^c$
UPDRS III at last assessment	26.0 ± 18.2	34.6 ± 22.0	51.5 ± 15.7	$F(2,20) = 3.4, P = 0.06$
Contralateral limb UPDRS III at last assessment	18.0 ± 13.1	24.7 ± 14.8	36.4 ± 10.7	$F(2,20) = 3.6, P = 0.05$
MMSE at SPECT	18.0 ± 3.2	18.9 ± 4.8	20.0 ± 5.7	$F(2,20) = 0.3, P = 0.8$
MMSE at last assessment	10.3 ± 5.5	10.9 ± 8.8	12.8 ± 6.2	$F(2,20) = 0.3, P = 0.8$
CAMCOG at SPECT	59.8 ± 10.2	65.7 ± 13.3	65.0 ± 17.0	$F(2,20) = 0.2, P = 0.8$
CAMCOG at last assessment	60.3 ± 11.5	59.7 ± 15.9	53.2 ± 18.2	$F(2,20) = 0.5, P = 0.6$

Values expressed as mean ± standard deviation.

Post hoc tests (Gabriel's):

a Alzheimer's disease > Parkinson's disease dementia ( $P = 0.02$ ).

b Parkinson's disease dementia > dementia with Lewy bodies ( $P = 0.04$ ).

c Parkinson's disease dementia > Alzheimer's disease ( $P = 0.002$ ).

Otherwise not significant.

CAMCOG = Cambridge Cognitive Examination; MMSE = Mini-Mental State Examination.

bodies ( $P \leq 0.03$ ). There were no significant correlations in any group between FP-CIT imaging measures and baseline age (absolute values  $|r| \leq 0.43, P \geq 0.32$ ), Cambridge Cognitive Examination ( $|r| \leq 0.46, P \geq 0.60$ ), Mini-Mental State Examination ( $|r| \leq 0.60, P \geq 0.32$ ) or UPDRS III ( $|r| \leq 0.34, P \geq 0.80$ ) scores.

## Substantia nigra and striatum neuropathology—right hemisphere

Table 2 presents a summary of nigral and striatal pathology measures for the cases with Alzheimer's disease, dementia with Lewy bodies and Parkinson's disease dementia. Test-retest reliability for nigral neuronal density,  $\alpha$ -synuclein and tau measurements were: intraclass correlation coefficient (95% CI): 0.98 (0.94–0.99), 0.86 (0.60–0.97) and 0.98 (0.96–0.99), respectively. Striatal (caudate, putamen)  $\alpha$ -synuclein, tau and amyloid  $\beta$  intraclass correlation coefficients (95% CI) were: [0.92 (0.74–0.98), 0.83 (0.58–0.97)], [0.90 (0.68–0.98), 0.94 (0.79–0.99)] and [0.99 (0.98–0.99), 0.98 (0.94–0.99)], respectively. Results indicate excellent reproducibility for neuropathological data.

There were no significant correlations in any group between the assessed neuropathological lesions (i.e. pigmented neuron density,  $\alpha$ -synuclein and tau) in the substantia nigra and age at death ( $|r| \leq 0.79, P \geq 0.12$ ), and last assessment measures of Cambridge Cognitive Examination ( $|r| \leq 0.74, P \geq 0.09$ ), Mini-Mental State Examination ( $|r| \leq 0.73, P \geq 0.09$ ) and UPDRS III (total and contralateral limb,  $|r| \leq 0.63, P \geq 0.21$ ). Similarly, no significant associations were found in any group between striatal pathology ( $\alpha$ -synuclein, tau and amyloid  $\beta$ ) and age at death ( $|r| \leq 0.79, P \geq 0.30$ ), and last assessment measures of

Cambridge Cognitive Examination ( $|r| \leq 0.66, P \geq 0.06$ ), Mini-Mental State Examination ( $|r| \leq 0.70, P \geq 0.24$ ) and UPDRS III (total and contralateral limb;  $|r| \leq 0.81, P \geq 0.18$ ). Pooling the groups ( $n = 23$ ), a significant correlation was observed between nigral neuronal number and degree of tau pathology ( $r = 0.59, P = 0.002$ ), which was not observed when calculated for Alzheimer's disease cases only ( $r = -0.55, P = 0.46$ ). A trend towards a negative correlation was also seen between nigral neuronal number and degree of  $\alpha$ -synuclein pathology ( $r = -0.39, P = 0.08$ ). For the pooled group, the relationship between nigral and striatal pathologies was also investigated. Nigral  $\alpha$ -synuclein and tau pathology were found not be associated with striatal  $\alpha$ -synuclein ( $|r| \leq 0.24, P \geq 0.52$ ), tau ( $|r| \leq 0.23, P \geq 0.60$ ) or amyloid  $\beta$  ( $|r| \leq 0.42, P \geq 0.06$ ) pathology.

## Neuropathological correlates of $^{123}\text{I}$ -FP-CIT single photon emission computed tomography binding—right hemisphere

To identify potential neuropathological predictors of  $^{123}\text{I}$ -FP-CIT SPECT binding across the entire study sample (Alzheimer's disease, dementia with Lewy bodies and Parkinson's disease dementia combined), individual stepwise regression analyses were performed for each  $^{123}\text{I}$ -FP-CIT uptake measure [caudate, anterior putamen, posterior putamen and whole striatum (including all three regions)] as the dependent variable, and nigral neuronal density as well as nigral and where appropriate caudate or putamen ( $\alpha$ -synuclein, tau and amyloid  $\beta$ ) pathologies as independent variables. The analysis revealed that neuronal density significantly

**Table 2** Summary of  $^{123}\text{I}$ -FP-CIT SPECT binding ratios and neuropathological measures in Alzheimer's disease, dementia with Lewy bodies and Parkinson's disease dementia

	Alzheimer's disease (n = 4)	Dementia with Lewy bodies (n = 7)	Parkinson's disease dementia (n = 12)	P-value
SPECT imaging—right hemisphere				
FP-CIT uptake				
Caudate	2.95 ± 0.29	2.99 ± 0.56	2.11 ± 0.63	$F(2,20) = 6.6, P = 0.006^a$
Anterior putamen	3.37 ± 0.92	2.82 ± 0.57	1.94 ± 0.65	$F(2,20) = 8.2, P = 0.003^a$
Posterior putamen	2.70 ± 0.89	2.06 ± 0.53	1.22 ± 0.19	$F(2,20) = 17.4, P < 0.001^a$
Striatum <sup>f</sup>	3.00 ± 0.65	2.62 ± 0.50	1.75 ± 0.45	$F(2,20) = 12.3, P < 0.001^a$
FP-CIT annual rate of decline, expressed as per cent of baseline value <sup>e</sup>				
Caudate	0.4 ± 5.9	− 5.9 ± 7.7	− 16.8 ± 8.9	$F(2,20) = 8.4, P = 0.002^b$
Anterior putamen	− 1.9 ± 2.0	− 7.2 ± 8.9	− 9.6 ± 10.4	$F(2,20) = 1.1, P = 0.4$
Posterior putamen	1.3 ± 5.0	− 9.0 ± 13.1	1.4 ± 9.2	$F(2,20) = 2.6, P = 0.1$
Striatum <sup>f</sup>	− 0.1 ± 4.3	− 7.4 ± 9.4	− 8.4 ± 6.0	$F(2,20) = 2.1, P = 0.2$
Neuropathology—right hemisphere				
Substantia nigra				
Neurons/mm <sup>2</sup>	129.8 ± 38.0	34.4 ± 27.0	24.2 ± 15.3	$F(2,20) = 30.8, P < 0.001^c$
α-synuclein	0	0.005 ± 0.004	0.005 ± 0.005	$F(1,17) = 0.06, P = 0.8$
Tau	0.082 ± 0.061	0.012 ± 0.008	0.007 ± 0.007	$F(2,20) = 14.7, P < 0.001^c$
Caudate				
α-synuclein	0	0.0056 ± 0.014	0.0021 ± 0.0022	$F(1,17) = 0.7, P = 0.4$
Tau	0.000049 ± 0.000094	0.0005 ± 0.001	0.0013 ± 0.0034	$F(2,20) = 0.4, P = 0.7$
Amyloid β	0.043 ± 0.015	0.028 ± 0.032	0.008 ± 0.011	$F(2,20) = 5.4, P = 0.01^d$
Putamen				
α-synuclein	0	0.0023 ± 0.002	0.0059 ± 0.0091	$F(1,17) = 1.1, P = 0.3$
Tau	0.0007 ± 0.0009	0.00034 ± 0.0009	0.00082 ± 0.0014	$F(2,20) = 0.3, P = 0.8$
Amyloid β	0.038 ± 0.009	0.020 ± 0.017	0.007 ± 0.010	$F(2,20) = 9.5, P = 0.001^d$

Values expressed as mean ± standard deviation.

Post hoc tests (Gabriel's):

a Alzheimer's disease > Parkinson's disease dementia, dementia with Lewy bodies > Parkinson's disease dementia ( $P \leq 0.04$ ).

b Parkinson's disease dementia > Alzheimer's disease, dementia with Lewy bodies ( $P \leq 0.03$ ).

c Alzheimer's disease > dementia with Lewy bodies, Alzheimer's disease > Parkinson's disease dementia ( $P \leq 0.001$ ).

d Alzheimer's disease > Parkinson's disease dementia ( $P \leq 0.02$ ).

Otherwise not significant.

e Data obtained from a previous longitudinal FP-CIT study of dementia (Colloby *et al.*, 2005).

f Calculated from the arithmetic mean of caudate, anterior and posterior putamen values.

predicted  $^{123}\text{I}$ -FP-CIT uptake in all regions ( $P \leq 0.04$ ), but not α-synuclein ( $P \geq 0.46$ ), tau ( $P \geq 0.18$ ) or amyloid β ( $P \geq 0.22$ ) burden. Neuronal density accounted for 20% of the variance in caudate [ $F(1,20) = 4.8, R^2 = 0.20, \text{amyloid } \beta = 0.45, P = 0.04$ ], 40% in anterior putamen [ $F(1,20) = 13.1, R^2 = 0.40, \text{amyloid } \beta = 0.63, P = 0.002$ ], 58% in posterior putamen [ $F(1,20) = 26.7, R^2 = 0.58, \text{amyloid } \beta = 0.76, P < 0.001$ ] and 45% in striatum [ $F(1,20) = 15.7, R^2 = 0.45, \text{amyloid } \beta = 0.66, P = 0.001$ ]. This suggests that in these cases, reduced striatal  $^{123}\text{I}$ -FP-CIT uptake was attributed to decreased dopaminergic neuronal density but not α-synuclein, tau or amyloid β pathology.

Partial correlation analysis was then used to examine the strength of association between neuronal density and  $^{123}\text{I}$ -FP-CIT SPECT uptake measures with and without controlling for the interval between SPECT scan and death, and  $^{123}\text{I}$ -FP-CIT per cent annual rate of decline. Table 3 presents both the zero order ( $r$ ) and partial ( $r'$ ) correlation coefficients and associated  $P$ -values where results were essentially similar for both analyses. Figure 3A–D illustrates scatter plots of binding ratios in caudate, anterior putamen, posterior putamen and striatum against

neuronal density across the entire study population. In addition, Fig. 4 shows axial  $^{123}\text{I}$ -FP-CIT SPECT scans with corresponding images of nigral dopaminergic neurons in selected cases with Alzheimer's disease and dementia with Lewy bodies.

## Discussion

This is the first study to examine the relationship between *in vivo* dopaminergic  $^{123}\text{I}$ -FP-CIT SPECT imaging and nigral and striatal neuropathology in a group comprising of autopsy-confirmed cases with Alzheimer's disease, dementia with Lewy bodies and Parkinson's disease dementia. Nigral neuronal density was found to be a significant predictor of  $^{123}\text{I}$ -FP-CIT uptake ratios in caudate, anterior and posterior putamen as well as striatum ( $P \leq 0.04$ ). However, nigral and striatal α-synuclein, tau and amyloid β pathologies were not significant predictors of striatal  $^{123}\text{I}$ -FP-CIT binding in these subjects ( $P \geq 0.18$ ). In addition, the correlation between  $^{123}\text{I}$ -FP-CIT uptake and neuronal density remained statistically significant even after accounting for the interval between

SPECT scan and death, and  $^{123}\text{I}$ -FP-CIT annual per cent rate of decline. The results are consistent with the view that dopaminergic cell loss in the substantia nigra pars compacta affects striatal dopaminergic function due to disturbances in the dopaminergic

**Table 3** Zero order ( $r$ ) and partial ( $r'$ ) correlation coefficients of relationship between  $^{123}\text{I}$ -FP-CIT SPECT uptake in each region of interest and dopaminergic neuronal density in substantia nigra for combined groups

SPECT imaging—right hemisphere	Neurons per $\text{mm}^2$ (zero order)	Neurons per $\text{mm}^2$ (partial) <sup>a</sup>
Caudate	$r = 0.43, P = 0.08$	$r' = 0.41, P = 0.12$
Anterior putamen	<b><math>r = 0.62, P = 0.004</math></b>	<b><math>r' = 0.61, P = 0.008</math></b>
Posterior putamen	<b><math>r = 0.74, P &lt; 0.001</math></b>	<b><math>r' = 0.76, P &lt; 0.001</math></b>
Striatum	<b><math>r = 0.65, P &lt; 0.001</math></b>	<b><math>r' = 0.66, P = 0.004</math></b>

Values expressed as correlation coefficients, corrected  $P$ -values.

Bold text denotes significant correlations.

<sup>a</sup>Controlling for interval between SPECT scan and death, and  $^{123}\text{I}$ -FP-CIT per cent annual rate of decline.

projections via the nigrostriatal pathways. Other structures may also be implicated, such as globus pallidus and subthalamic nucleus, which express a significant pathological burden that may also contribute to the observed striatal dopaminergic dysfunction.

Walker and colleagues (2007), investigated whether FP-CIT imaging improved the accuracy in diagnosing dementia with Lewy bodies from non-dementia with Lewy bodies compared with clinical criteria alone using autopsy-confirmed diagnosis as the 'gold' standard. They showed that sensitivity increased to 88% (75% clinical) and specificity to 100% (42% clinical) when using FP-CIT scans. However, results from their and our studies reveal a small number of false-negative scans in patients with the clinicopathological diagnosis of dementia with Lewy bodies. These individuals may express cortical and striatal Lewy body pathology without significant nigrostriatal neuronal loss. This can be demonstrated in Fig. 3, where the highlighted cases with dementia with Lewy bodies with a visual rating of 'normal' uptake (O'Brien *et al.*, 2004) exhibited a greater level of nigral neurons that were distinct from the rest of the dementia with Lewy bodies cohort (subjects with 'abnormal' uptake on visual rating).

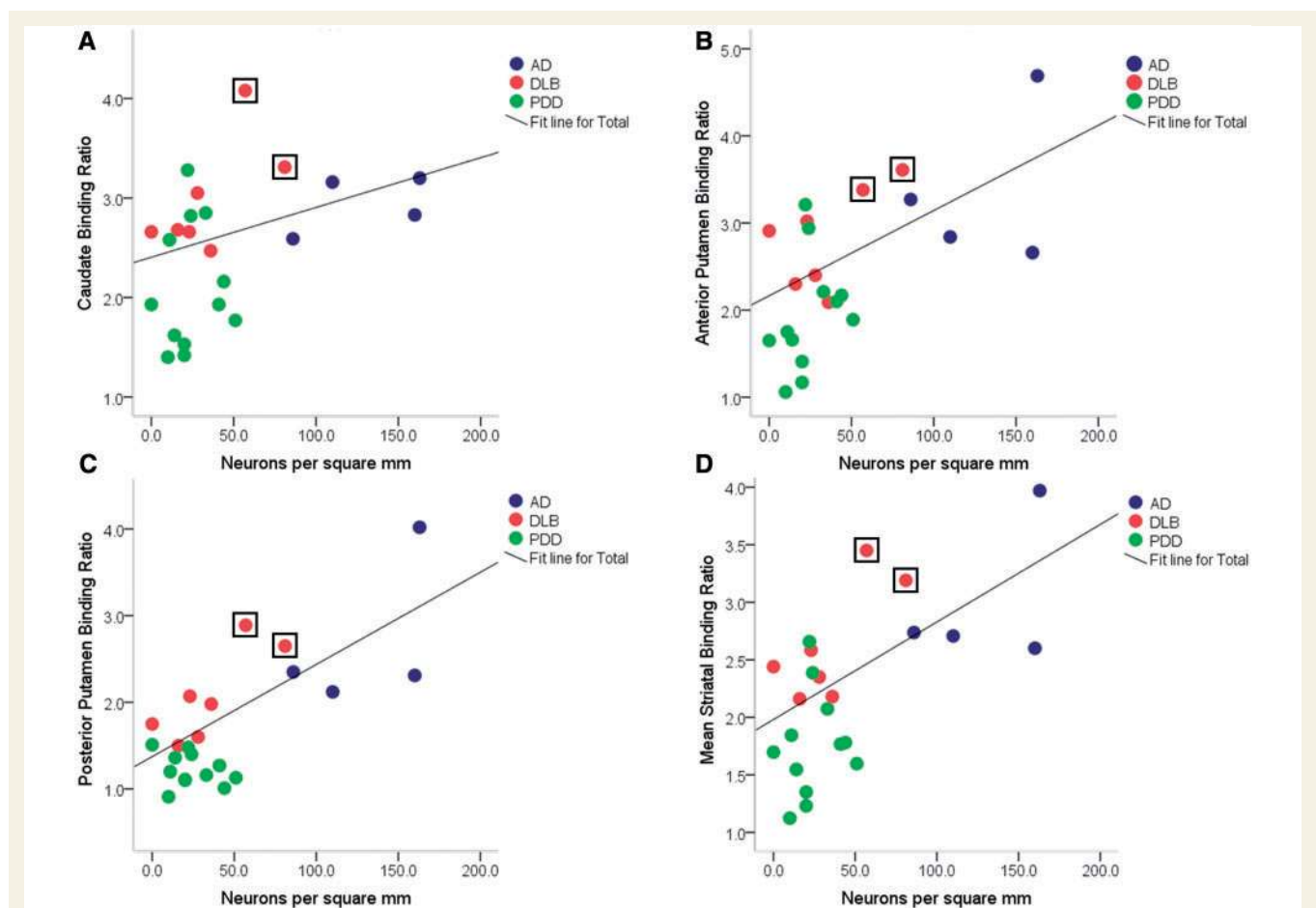


**Figure 3** Scatter plots of binding ratios in caudate (A), anterior putamen (B), posterior putamen (C) and striatum (D) against neuronal density in substantia nigra (data for right hemisphere) across Alzheimer's disease (AD), dementia with Lewy bodies (DLB) and Parkinson's disease dementia (PDD) groups. Boxed cases represent subjects with dementia with Lewy bodies with a visual rating of 'normal' FP-CIT uptake.



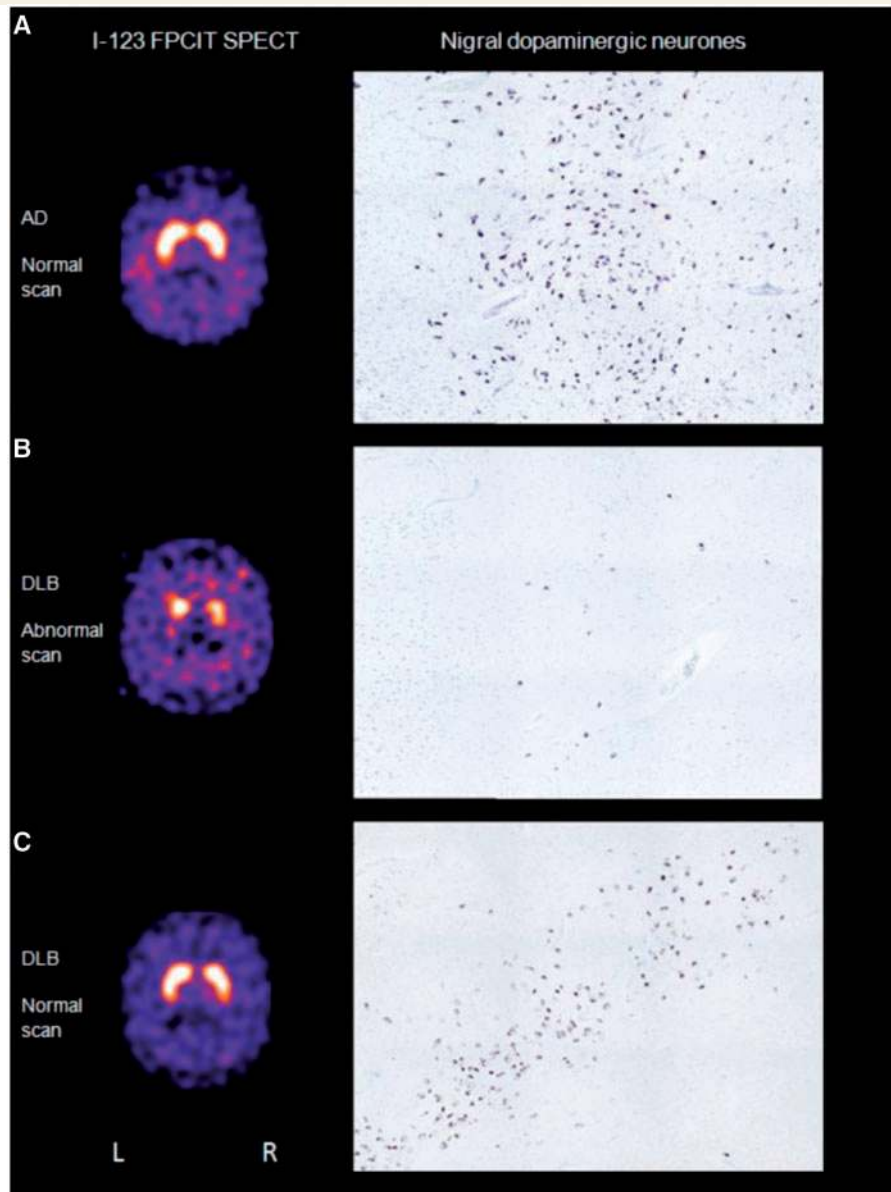


**Figure 4** Axial  $^{123}\text{I}$ -FP-CIT SPECT scans with corresponding images of nigral dopaminergic neurons. (A) Subject with Alzheimer's disease (AD) with a 'grade 0—normal' FP-CIT scan and nigral density of 160 neurons per  $\text{mm}^2$ . (B) Subject with dementia with Lewy bodies (DLB) with a 'grade 2—abnormal' FP-CIT scan and nigral density of 16 neurons per  $\text{mm}^2$ . (C) Subject with dementia with Lewy bodies with a 'grade 0—normal' FP-CIT scan and nigral density of 81 neurons per  $\text{mm}^2$ . Note, FP-CIT SPECT scans are displayed neurologically (left on left side, L = left, R = right).

Functional and structural imaging changes in striatum have been demonstrated in Alzheimer's disease, dementia with Lewy bodies and Parkinson's disease dementia. Evidence from SPECT and PET imaging region of interest studies suggests that striatal dopaminergic deficits are associated with dementia with Lewy bodies and Parkinson's disease dementia (Donnemiller *et al.*, 1997; Hu *et al.*, 2000; Ito *et al.*, 2002; Walker *et al.*, 2002; O'Brien *et al.*, 2004; Koeppe *et al.*, 2008). Using voxel-based methods, Lee *et al.* (2010) showed that grey matter density was significantly decreased in putamen bilaterally in dementia with Lewy bodies but not in Parkinson's disease dementia compared with controls, while others revealed grey matter volume loss in right caudate and

putamen in Parkinson's disease dementia relative to controls and no differences in grey matter volume between dementia with Lewy bodies and Parkinson's disease dementia (Burton *et al.*, 2004). More recently, another study showed that grey matter volume loss in right caudate was associated with dementia with Lewy bodies (Watson *et al.*, 2012). Using region of interest procedures, volumetric loss in putamen has also been reported bilaterally in dementia with Lewy bodies compared with Alzheimer's disease and controls (Cousins *et al.*, 2003), while caudate atrophy has been observed in Alzheimer's disease and dementia with Lewy bodies but not in Parkinson's disease dementia (Barber *et al.*, 2002; Almeida *et al.*, 2003).

Although we found an association between  $^{123}\text{I}$ -FP-CIT uptake and nigrostriatal neuronal loss, we did not find an association between  $^{123}\text{I}$ -FP-CIT uptake and nigral or striatal  $\alpha$ -synuclein. This potentially challenges the specificity of *in vivo* dopaminergic imaging as a predictor of  $\alpha$ -synuclein *per se*. However,  $\alpha$ -synuclein and not tau burden showed a trend towards a negative correlation with the number of nigral neurons. This suggests a reduction of nigral neurons occurs in Lewy body diseases but not in Alzheimer's disease, even with considerable amounts of nigral tau pathology. This is further supported by the significant positive correlation between tau pathology and nigral neuronal number in the whole study cohort. Lewy body dementia cases that virtually lack tau pathology had considerable nigral neuronal loss whereas Alzheimer's disease cases with nigral tau pathology had a greater number of nigral neurons. Therefore our results are consistent with previous studies indicating the feasibility of  $^{123}\text{I}$ -FP-CIT SPECT in distinguishing dementia with Lewy bodies/Parkinson's disease dementia from Alzheimer's disease (O'Brien *et al.*, 2004, 2009). Of note, our study cohort consisted of dementia with Lewy bodies/patients with Parkinson's disease dementia with and patients with Alzheimer's disease without extrapyramidal symptoms, respectively. We have shown previously (Attems *et al.*, 2007) that in patients with Alzheimer's disease extrapyramidal symptoms were associated with nigral cell loss that statistically correlated with both nigral  $\alpha$ -synuclein and tau pathology (semi-quantitative assessments). However, as nigral tau pathology was frequently present in cases with Alzheimer's disease without extrapyramidal symptoms, only  $\alpha$ -synuclein pathology correlated with the presence of extrapyramidal symptoms suggesting that semi-quantitative assessment in this cohort might have biased statistical analyses regarding associations between nigral cell loss and tau pathology. Moreover, Ceravolo *et al.* (2004) found striatal  $^{123}\text{I}$ -FP-CIT uptake in patients with Alzheimer's disease with parkinsonism to be similar to controls and significantly higher than both dementia with Lewy bodies and Parkinson's disease. These findings indicate that nigral cell loss is closely linked to  $\alpha$ -synuclein pathology. Reduced striatal  $^{123}\text{I}$ -FP-CIT uptake may indeed be a surrogate marker of nigral and striatal  $\alpha$ -synuclein burden, and the lack of a significant correlation observed between  $^{123}\text{I}$ -FP-CIT uptake and  $\alpha$ -synuclein pathology may be a consequence of reduced statistical power due to the relatively small sample, which is a limitation of the present study. Further studies on the relationship between striatal  $^{123}\text{I}$ -FP-CIT uptake and nigral pathology assessed by quantitative methods in cases with Alzheimer's disease with and cases with dementia with Lewy bodies without extrapyramidal symptoms are also warranted to elucidate the potential of striatal  $^{123}\text{I}$ -FP-CIT uptake in the prediction of nigral  $\alpha$ -synuclein pathology.

In conclusion, nigral dopaminergic cell loss rather than  $\alpha$ -synuclein, tau or amyloid  $\beta$  pathology was associated with decreased striatal  $^{123}\text{I}$ -FP-CIT binding in an autopsy-confirmed group of subjects with Alzheimer's disease, dementia with Lewy bodies and Parkinson's disease dementia. This suggests that reduced uptake *in vivo* may be influenced considerably by neuronal loss rather than the presence of pathological lesions, although dysfunctional nigral neurons may have an additional effect on

striatal uptake *in vivo* but their respective role remains to be elucidated.

## Acknowledgements

The authors thank staff at the Regional Medical Physics Department, Newcastle General Hospital, for undertaking SPECT scanning and all members of the Lewy body research team who helped with patient recruitment and assessment.

## Funding

Medical Research Council for financial support and GE Healthcare for provision of the FP-CIT ligand used in this study. This work was supported by the UK NIHR Biomedical Research Centre for Ageing and Age-Related Disease and the Biomedical Research Unit for Lewy body dementia awards to the Newcastle upon Tyne Hospitals NHS Foundation Trust. Part of this study was supported by the Dunhill Medical Trust (R173/1110). Tissue for this study was provided by the Newcastle Brain Tissue Resource, which is funded in part by a grant from the UK Medical Research Council (G0400074).

## References

- Aarsland D, Perry R, Brown A, Larsen JP, Ballard C. Neuropathology of dementia in Parkinson's disease: a prospective, community-based study. *Ann Neurol* 2005; 58: 773–6.
- Alafuzoff I, Ince PG, Arzberger T, Al-Sarraj S, Bell J, Bodi I, et al. Staging/typing of Lewy body related alpha-synuclein pathology: a study of the BrainNet Europe Consortium. *Acta Neuropathol* 2009; 117: 635–52.
- Almeida OP, Burton EJ, McKeith I, Gholkar A, Burn D, O'Brien JT. MRI study of caudate nucleus volume in Parkinson's disease with and without dementia with Lewy bodies and Alzheimer's disease. *Dement Geriatr Cogn Disord* 2003; 16: 57–63.
- Attems J, Quass M, Jellinger KA. Tau and alpha-synuclein brainstem pathology in Alzheimer disease: relation with extrapyramidal signs. *Acta Neuropathol* 2007; 113: 53–62.
- Attems J, Thomas A, Jellinger K. Correlations between cortical and sub-cortical tau pathology. *Neuropathol Appl Neurobiol* 2011. Advance Access published on November 24, (2011), doi: 10.1111/j.1365-2990.2011.01244.x.
- Barber R, McKeith I, Ballard C, O'Brien J. Volumetric MRI study of the caudate nucleus in patients with dementia with Lewy bodies, Alzheimer's disease, and vascular dementia. *J Neurol Neurosurg Psychiatry* 2002; 72: 406–7.
- Braak H, Alafuzoff I, Arzberger T, Kretschmar H, Del Tredici K. Staging of Alzheimer disease-associated neurofibrillary pathology using paraffin sections and immunocytochemistry. *Acta Neuropathol* 2006; 112: 389–404.
- Braak H, Del Tredici K, Rub U, de Vos RA, Jansen Steur EN, Braak E. Staging of brain pathology related to sporadic Parkinson's disease. *Neurobiol Aging* 2003; 24: 197–211.
- Burton EJ, McKeith IG, Burn DJ, Williams ED, O'Brien JT. Cerebral atrophy in Parkinson's disease with and without dementia: a comparison with Alzheimer's disease, dementia with Lewy bodies and controls. *Brain* 2004; 127: 791–800.
- Burton EJ, Mukaetova-Ladinska EB, Perry RH, Jaros E, Barber R, O'Brien JT. Neuropathological correlates of volumetric MRI in

- autopsy-confirmed Lewy body dementia. *Neurobiol Aging* 2012; 33: 1228–36.
- Ceravolo R, Volterrani D, Gambaccini G, Bernardini S, Rossi C, Logi C, et al. Presynaptic nigro-striatal function in a group of Alzheimer's disease patients with parkinsonism: evidence from a dopamine transporter imaging study. *J Neural Transm* 2004; 111: 1065–73.
- Colloby SJ, Williams ED, Burn DJ, Lloyd JJ, McKeith IG, O'Brien JT. Progression of dopaminergic degeneration in dementia with Lewy bodies and Parkinson's disease with and without dementia assessed using (123I)-FP-CIT SPECT. *Eur J Nucl Med Mol Imaging* 2005; 32: 1176–85.
- Cousins DA, Burton EJ, Burn D, Gholkar A, McKeith IG, O'Brien JT. Atrophy of the putamen in dementia with Lewy bodies but not Alzheimer's disease: an MRI study. *Neurology* 2003; 61: 1191–5.
- Csernansky JG, Hamstra J, Wang L, McKeel D, Price JL, Gado M, et al. Correlations between antemortem hippocampal volume and postmortem neuropathology in AD subjects. *Alzheimer Dis Assoc Disord* 2004; 18: 190–5.
- Donnemiller E, Heilmann J, Wenning GK, Berger W, Decristoforo C, Moncayo R, et al. Brain perfusion scintigraphy with 99mTc-HMPAO or 99mTc-ECD and 123I-beta-CIT single-photon emission tomography in dementia of the Alzheimer-type and diffuse Lewy body disease. *Eur J Nucl Med Mol Imaging* 1997; 24: 320–5.
- Duda JE, Giasson BI, Mabon ME, Lee VM, Trojanowski JQ. Novel antibodies to synuclein show abundant striatal pathology in Lewy body diseases. *Ann Neurol* 2002; 52: 205–10.
- Duyckaerts C, Delatour B, Potier MC. Classification and basic pathology of Alzheimer disease. *Acta Neuropathol* 2009; 118: 5–36.
- Emre M, Aarsland D, Brown R, Burn DJ, Duyckaerts C, Mizuno Y, et al. Clinical diagnostic criteria for dementia associated with Parkinson's disease. *Mov Disord* 2007; 22: 1689–707; quiz 837.
- Fahn S, Elton RL, Marsden CD, Goldstein M. Unified Parkinson's disease rating scale. Recent developments in Parkinson's disease. New Jersey: Macmillan; 1987. p. 153–63.
- Ferman TJ, Boeve BF. Dementia with Lewy bodies. *Neurol Clin* 2007; 25: 741–60, vii.
- Folstein MF, Folstein SE, McHugh PR. "Mini-mental state". A practical method for grading the cognitive state of patients for the clinician. *J Psychiatr Res* 1975; 12: 189–98.
- Gosche KM, Mortimer JA, Smith CD, Markesbery WR, Snowdon DA. Hippocampal volume as an index of Alzheimer neuropathology: findings from the Nun Study. *Neurology* 2002; 58: 1476–82.
- Hamilton RL. Lewy bodies in Alzheimer's disease: a neuropathological review of 145 cases using alpha-synuclein immunohistochemistry. *Brain Pathol (Zurich, Switzerland)* 2000; 10: 378–84.
- Hu XS, Okamura N, Arai H, Higuchi M, Matsui T, Tashiro M, et al. F-18-fluorodopa PET study of striatal dopamine uptake in the diagnosis of dementia with Lewy bodies. *Neurology* 2000; 55: 1575–6.
- Huesgen CT, Burger PC, Crain BJ, Johnson GA. In vitro MR microscopy of the hippocampus in Alzheimer's disease. *Neurology* 1993; 43: 145–52.
- Hurtig HI, Trojanowski JQ, Galvin J, Ewbank D, Schmidt ML, Lee VM, et al. Alpha-synuclein cortical Lewy bodies correlate with dementia in Parkinson's disease. *Neurology* 2000; 54: 1916–21.
- Hyman BT. New neuropathological criteria for Alzheimer disease. *Arch Neurol* 1998; 55: 1174–6.
- Ito K, Nagano-Saito A, Kato T, Arahata Y, Nakamura A, Kawasumi Y, et al. Striatal and extrastriatal dysfunction in Parkinson's disease with dementia: a 6- F-18 fluoro-L-dopa PET study. *Brain* 2002; 125: 2144.
- Jack CR Jr., Dickson DW, Parisi JE, Xu YC, Cha RH, O'Brien PC, et al. Antemortem MRI findings correlate with hippocampal neuropathology in typical aging and dementia. *Neurology* 2002; 58: 750–7.
- Koeppel RA, Gilman S, Junck L, Wernette K, Frey KA. Differentiating Alzheimer's disease from dementia with Lewy bodies and Parkinson's disease with (+)-[11C]dihydrotrabenazine positron emission tomography. *Alzheimer's & dementia: the journal of the Alzheimer's Association* 2008; 4: S67–76.
- Lee JE, Park B, Song SK, Sohn YH, Park HJ, Lee PH. A comparison of gray and white matter density in patients with Parkinson's disease dementia and dementia with Lewy bodies using voxel-based morphometry. *Mov Disord* 2010; 25: 28–34.
- Libow LS, Frisina PG, Haroutunian V, Perl DP, Purohit DP. Parkinson's disease dementia: a diminished role for the Lewy body. *Parkinsonism Relat Disord* 2009; 15: 572–5.
- McKeith IG, Dickson DW, Lowe J, Emre M, O'Brien JT, Feldman H, et al. Diagnosis and management of dementia with Lewy bodies: third report of the DLB Consortium. *Neurology* 2005; 65: 1863–72.
- McKeith IG, Galasko D, Kosaka K, Perry EK, Dickson DW, Hansen LA, et al. Consensus guidelines for the clinical and pathologic diagnosis of dementia with Lewy bodies (DLB): report of the consortium on DLB international workshop. *Neurology* 1996; 47: 1113–24.
- McKhann G, Drachman D, Folstein M, Katzman R, Price D, Stadlan EM. Clinical diagnosis of Alzheimer's disease: report of the NINCDS-ADRDA Work Group under the auspices of Department of Health and Human Services Task Force on Alzheimer's Disease. *Neurology* 1984; 34: 939–44.
- Mirra SS, Hart MN, Terry RD. Making the diagnosis of Alzheimer's disease. A primer for practicing pathologists. *Arch Pathol Lab Med* 1993; 117: 132–44.
- Nicola SM, Surmeier J, Malenka RC. Dopaminergic modulation of neuronal excitability in the striatum and nucleus accumbens. *Ann Rev Neurosci* 2000; 23: 185–215.
- O'Brien JT, Colloby SJ, Fenwick J, Williams ED, Firbank M, Burn D, et al. Dopamine transporter loss visualized with FP-CIT SPECT in the differential diagnosis of dementia with Lewy bodies. *Arch Neurol* 2004; 61: 919–25.
- O'Brien JT, McKeith IG, Walker Z, Tatsch K, Booij J, Darcourt J, et al. Diagnostic accuracy of 123I-FP-CIT SPECT in possible dementia with Lewy bodies. *Br J Psychiatry* 2009; 194: 34–9.
- Perl DP. Neuropathology of Alzheimer's disease. New York: *Mt Sinai J 100 Med*; 2010; 77: 32–42.
- Rahkonen T, Eloniemi-Sulkava U, Rissanen S, Vatanen A, Viramo P, Sulkava R. Dementia with Lewy bodies according to the consensus criteria in a general population aged 75 years or older. *J Neurol Neurosurg Psychiatry* 2003; 74: 720–4.
- Roth M, Tym E, Mountjoy CQ, Huppert FA, Hendrie H, Verma S, et al. CAMDEX. A standardised instrument for the diagnosis of mental disorder in the elderly with special reference to the early detection of dementia. *Br J Psychiatry* 1986; 149: 698–709.
- Sahin HA, Emre M, Ziabreva I, Perry E, Celasun B, Perry R. The distribution pattern of pathology and cholinergic deficits in amygdaloid complex in Alzheimer's disease and dementia with Lewy bodies. *Acta Neuropathol* 2006; 111: 115–25.
- Samuel W, Galasko D, Masliah E, Hansen LA. Neocortical lewy body counts correlate with dementia in the Lewy body variant of Alzheimer's disease. *J Neuropathol Exp Neurol* 1996; 55: 44–52.
- Schulz-Schaeffer WJ. The synaptic pathology of alpha-synuclein aggregation in dementia with Lewy bodies, Parkinson's disease and Parkinson's disease dementia. *Acta Neuropathol* 2010; 120: 131–43.
- Tsuboi Y, Uchikado H, Dickson DW. Neuropathology of Parkinson's disease dementia and dementia with Lewy bodies with reference to striatal pathology. *Parkinsonism Relat Disord* 2007; 13: S221–4.
- Walker Z, Costa DC, Walker RWH, Shaw K, Gacinovic S, Stevens T, et al. Differentiation of dementia with Lewy bodies from Alzheimer's disease using a dopaminergic presynaptic ligand. *J Neurol Neurosurg Psychiatry* 2002; 73: 134–40.
- Walker Z, Jaros E, Walker RW, Lee L, Costa DC, Livingston G, et al. Dementia with Lewy bodies: a comparison of clinical diagnosis, FP-CIT single photon emission computed tomography imaging and autopsy. *J Neurol Neurosurg Psychiatry* 2007; 78: 1176–81.
- Watson R, O'Brien JT, Barber R, Blamire AM. Patterns of gray matter atrophy in dementia with Lewy bodies: a voxel-based morphometry study. *Int Psychogeriatr* 2012; 24: 532–40.